Annu. Rev. Astron. Astrophys. 1997. 35:607–36

PARSEC-SCALE JETS IN EXTRAGALACTIC RADIO SOURCES[1]

J. Anton Zensus
National Radio Astronomy Observatory,[2] Charlottesville, Virginia 22903

KEY WORDS: compact radio sources, radio source morphology, radio jets, VLBI jets, superluminal motion, jet models

ABSTRACT

Observations of parsec-scale radio jets associated with active galactic nuclei are reviewed, with a particular emphasis on high-luminosity core-dominated sources where the most detailed information on individual objects exists. Extensive imaging surveys with very long baseline interferometry (VLBI) have made possible a morphologic classification of compact radio sources and systematic studies of the statistics of apparent (often faster-than-light) motions found in an increasing number of sources. VLBI monitoring studies at centimeter and millimeter wavelengths, enhanced by spectral and polarization imaging, of representative types of AGN can discriminate detailed physical models. The observations are especially discussed in light of the variant of the relativistic beaming model that explains kinematic, spectral, and polarization properties of parsec-scale jets through shocks in an underlying continuous jet flow.

INTRODUCTION

The radio emission from radio-loud active galactic nuclei (AGN) ordinarily takes the form of collimated "jets" that connect a compact central region with kiloparsec-scale extended lobes and hot spots. For the past two decades, the structure and emission properties of these jets have been studied extensively

[2]The National Radio Astronomy Observatory is a facility of the National Science Foundation, operated under cooperative agreement by Associated Universities, Inc.

with aperture synthesis radio imaging (see Bridle & Perley 1984, Bridle 1996). Very long baseline interferometry (VLBI) has become the primary tool to probe the most compact of these emission regions with angular resolution of 0.1 to 2 milliarcsec, corresponding to linear scales of 0.2 to 10 parsec (pc) (see Zensus & Pearson 1990, Pearson 1996).

The direct radio imaging of parsec-scale jets and the complementary study of activity in the associated AGN in all spectral regimes has broadly impacted our understanding of these objects; in particular, they have inspired and constrained the development of realistic physical models, helped to establish the relativistic jet paradigm, and influenced the thinking about general AGN unification, radio source evolution, and cosmology.

The relativistic jet model (e.g. Blandford & Königl 1979) has become the de facto generally current AGN paradigm; it postulates that AGN are fueled by a massive central black hole and accretion disk at the base of a relativistic flow in symmetric twin jets (Rees 1971, Scheuer 1974, Blandford & Rees 1974). This scenario is rooted in the ideas that the source characteristics are determined by relativistic beaming (Shklovskii 1963), by relativistic injection from galactic nuclei (Rees 1966), and by accretion of matter on a central black hole (see Begelman et al 1984); the inner jets themselves are thought to be formed magnetically from a rapidly rotating accretion disk around the black hole (Blandford & Payne 1982). The only direct evidence for the existence of bulk relativistic outflow along the radio jets comes from the detection of collimated, apparent faster-than-light ("superluminal"), outward-motion of parsec-scale jets (see Readhead 1993, Zensus & Pearson 1987). The discovery of a rapidly rotating molecular disk in NGC 4258 arguably is the most direct demonstration of the presence of a black hole in the nucleus of an active galaxy (Miyoshi et al 1995, Moran et al 1995, but see also Burbidge & Burbidge 1997). The intraday variability found in a number of compact sources hints at the presence of linear dimensions for ultra-compact jet components that are smaller than light hours (see Wagner & Witzel 1995).

The radio radiation from parsec-scale extragalactic radio sources is partially transparent synchrotron emission with characteristic spectral and polarization properties, as well as significant inverse-Compton emission (see Marscher 1990, Hughes & Miller 1991). The flat spectra of compact sources can be explained by superposition of the synchrotron spectra of the individual components that form the compact structure, the compact base of the jet, and the bright regions within the jet flow. The details of the formation of inner jets that connect the nucleus to the observed radio jet, their acceleration to near the speed of light, and the strong collimation remain poorly understood (e.g. Marscher 1995, Begelman 1995). On the other hand, considerable progress has been made in explaining the kinematic, spectral, and polarization properties of parsec-scale

jets through shocks in an underlying continuous jet flow (Blandford & Königl 1979, Marscher & Gear 1985, Hughes et al 1989a). Simulations of hydro- and magneto-hydrodynamic relativistic jets have reached a quality where meaningful comparisons between numerical and observed jet properties and evolution are possible (see Wiita 1996, Norman 1996).

In the basic beaming model scenario, superluminal motion and morphologic differences in general between compact and extended radio sources are attributed to beaming and orientation effects; compact sources are thought to be basically extended lobe sources at a small inclination to the line of sight and with strongly Doppler boosted core flux density (Orr & Browne 1982). A unification of Seyfert galaxies of type 1 with type 2 is supported by optical studies of the polarization properties of broad- and narrow line regions (Antonucci 1993, Miller 1995). The original unification hypothesis for radio sources has also been extended and refined by adding opaque nuclear obscuring tori to the relativistic jets. Beamed, intermediate, and unbeamed populations of radio-moderate edge-darkened Fanaroff & Riley Class 1 galaxies and of radio-loud edge-brightened Class 2 galaxies have been identified (see Barthel 1989, 1995, Gopal-Krishna 1995, Urry & Padovani 1995). In particular, lobe-dominated, narrow-line radio galaxies such as Cygnus A are assumed to be the unbeamed counterparts to core-dominated, variable, and superluminal quasars like 3C 345; the FR I radio galaxies in turn are thought to be the unbeamed pendants to BL Lac type objects.

The observational study of parsec-scale jets has seen astonishing progress since early imagery of compact radio sources at milliarcsecond resolution was achieved with very long baseline interferometry (VLBI) (see Kellermann & Pauliny-Toth 1981). Extensive VLBI surveys (see Wilkinson 1995) have made possible a morphologic classification of compact radio sources (see Pearson 1996). The systematic measurement of motion in these large samples yields apparent velocity statistics and distribution of Lorentz factors that can be compared to other indicators of relativistic motion (see Ghisellini et al 1993, Vermeulen 1995). The surveys also provide clues for unification models and for cosmology (see Vermeulen 1995, Kellermann 1993, Gurvits 1994). Realistic physical models can be tested and constrained through in-depth studies of prototypical objects, in particular when VLBI observations are combined with information from other spectral regimes.

Advances in VLBI techniques have been especially successful in the areas of detailed long-term monitoring observations, multifrequency and polarization imaging, and sensitivity-enhancing phase referencing (see the reviews in Zensus et al 1995b). High-quality VLBI observations have become routinely possible, especially with the very long baseline array (VLBA) (Napier et al 1994). This versatile and dedicated instrument offers full polarization and spectral-line

imaging capability, as well as spectral coverage from 300 MHz to 45 GHz. Independent regional VLBI networks in the northern and southern hemispheres, coordinated global VLBI campaigns between the VLBA and the European VLBI Network, and the "World Array" campaigns have made possible images of outstanding fidelity (see Schilizzi 1995). At millimeter wavelengths, ad hoc arrays have been operating that result in images with submilliarcsecond resolution (Kirchbaum et al 1994b, Schalinski et al 1994, Bååth 1994). The first true space VLBI mission, the Japanese VLBI Space Observatory Programme (VSOP), launched in early 1997, should provide high-fidelity images of strong sources (>1 Jansky) at even greater resolution (Hirabayashi 1996).

This review summarizes observational properties of parsec-scale radio jets in extragalactic sources, focusing in particular on the high-luminosity core-dominated sources where the most detailed information on individual jets has been gathered. Recent accounts can also be found in several conference proceedings (Zensus & Kellermann 1994, Cohen & Kellermann 1995, Hardee et al 1996, Ekers et al 1996). Complementary perspectives are offered by Readhead (1993), Pearson (1996), Cawthorne (1991), Marscher (1995). A Hubble constant of $H_0 = 100\ h$ km s^{-1}Mpc^{-1}, a deceleration parameter $q_0 = 0.5$, and a spectral index definition $S_\nu \propto \nu^\alpha$ are assumed throughout this paper.

MORPHOLOGY

Flux-density limited radio sky surveys at short centimeter (e.g. 6 cm) wavelengths yield roughly equal numbers of steep-spectrum extended double-lobed sources and flat-spectrum objects that are unresolved on an arcsecond scale. Among these radio-loud objects, the flat-spectrum sources typically can be associated with blazars and quasars, whereas the steep-spectrum sources tend to be FR I or FR II radio galaxies. Parsec-scale jets are found in all types of powerful radio sources, although they occur predominantly in elliptical galaxies rather than in spirals (e.g. Seyferts, Liners). A classification based on overall radio size and morphology has become possible through VLBI surveys, which yield several major classes with distinct characteristics (see Wilkinson 1995, Pearson 1996): (*a*) luminous core-dominated flat-spectrum sources, (*b*) powerful double-lobed radio galaxies with hotspots (Fanaroff-Riley class II, FR II), (*c*) weaker double-lobed radio galaxies without leading hot spots (FR I types), (*d*) compact steep-spectrum sources (CSS sources), and (*e*) compact symmetric objects (CSOs). Figure 1 shows representative examples of compact source

Figure 1 Examples of VLBI structures of compact sources at 15 GHz (from JA Zensus, KI Kellerman, RC Vermeulen & MH Cohen, in preparation).

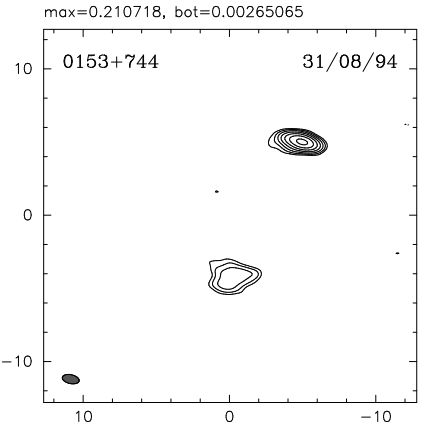
max=0.210718, bot=0.00265065
0153+744
31/08/94
10
0
−10
10
0
−10

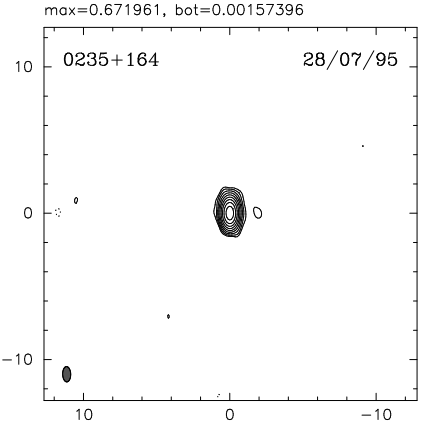
max=0.671961, bot=0.00157396
0235+164
28/07/95
10
0
−10
10
0
−10

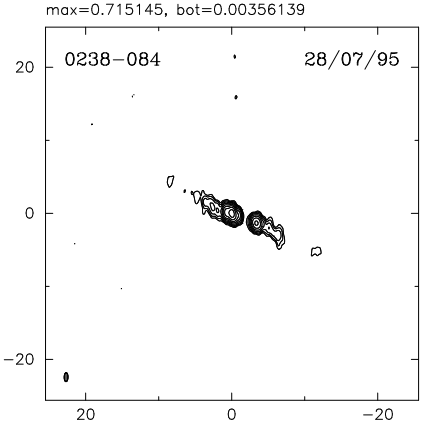
max=0.715145, bot=0.00356139
0238−084
28/07/95
20
0
−20
20
0
−20

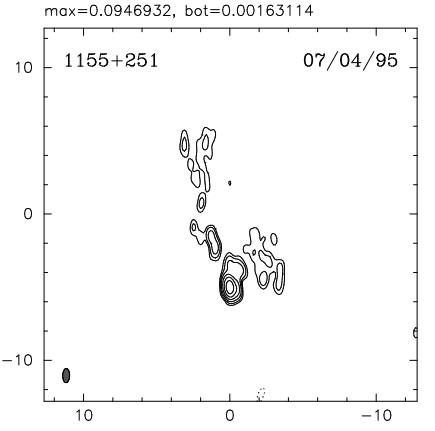
max=0.0946932, bot=0.00163114
1155+251
07/04/95
10
0
−10
10
0
−10

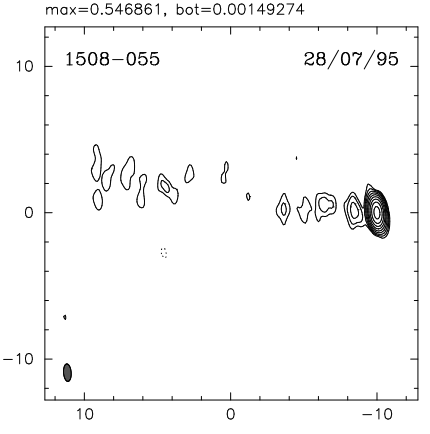
max=0.546861, bot=0.00149274
1508−055
28/07/95
10
0
−10
10
0
−10

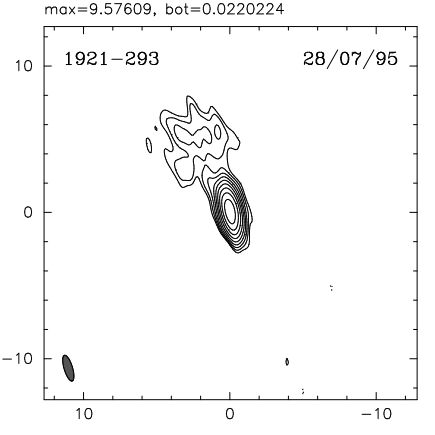
max=9.57609, bot=0.0220224
1921−293
28/07/95
10
0
−10
10
0
−10

structure typically found in high-frequency VLBI surveys (e.g. the 15 GHz survey of JA Zensus, KI Kellermann, RC Vermeulen & MH Cohen, in preparation). A range of astronomical phenomena has been attributed in part to gravitational lensing, and this effect has been suggested to be responsible for some of the distinguishing properties of AGN. Several of the known lens systems have VLBI jets, and their study reflects on the physics of AGN: For example, it can provide limits on source size (see Hewitt 1995).

High-Luminosity Core Dominated Objects

The high-luminosity core dominated objects are typically found in systematic flux-density–limited surveys of compact sources (see Wilkinson 1995 for a comprehensive review, Pearson & Readhead 1988, Witzel et al 1988, Wehrle et al 1992, Polatidis et al 1995, Thakkar et al 1995, Xu et al 1995, Taylor et al 1994, Henstock et al 1995). Such surveys are biased towards selecting strongly beamed objects, and indeed a majority (about 80–90%) have "core-jet" type structures, i.e. they contain an unresolved flat-spectrum "core" and a steeper-spectrum one-sided "jet" that in turn may contain distinct structure "components."

The cores are identified based on their compactness, flat or inverted radio spectra, and sometimes their flux density variability. In several cases, phase referencing observations have demonstrated little or no discernible movement for the core component, including 3C 345 (Bartel et al 1986), 1038+528 (Marcaide et al 1994b) and 4C39.25 (Guirado et al 1995). Narrow collimated jets are typical in this class of source.

The degree of alignment between these parsec-scale and the kiloparsec-scale jets shows a bimodal distribution with peaks near 0° and 90°, and BL Lac objects appear to show systematically stronger misalignments than quasars (e.g. Pearson & Readhead 1988, Wehrle et al 1992, Xu et al 1994, Appl et al 1996). This cannot be explained by a single population of slightly distorted jets, but it requires the presence of a second population of sources with small Lorentz factors and intrinsically large bending. Helical motion, perhaps arising in a binary black hole system, provides a likely mechanism to explain some cases that have been studied in detail (e.g. O'Dea et al 1988, Conway & Wrobel 1995). It is not yet clear if this is applicable for the population as a whole (Conway & Murphy 1993, Appl et al 1996), nor is it clear what causes the systematic differences found for BL Lac objects and quasars, of which the former have on average stronger misalignments (Conway & Murphy 1993, Conway 1994).

Structural variability and in particular apparent superluminal motion are frequently observed, and bulk relativistic motion is commonly inferred (Witzel et al 1988, Vermeulen 1995). Many of the observed jets are curved, and in some cases semioscillating trajectories or ridge lines have been observed (see below).

This effect is typically most pronounced near the core (Krichbaum & Witzel 1992).

A good example for a parsec-scale jet in a core-dominated source is the quasar 3C 345. Figure 2 shows an image at 5 GHz (Lobanov & Zensus 1997). This source has been regularly monitored with VLBI since 1979 (Biretta et al 1986, Zensus et al 1995a, Brown et al 1994, Wardle et al 1994, Rantakyrö et al 1995, Zensus et al 1995c). At 5 GHz, the jet appears continuous, but from comparison with images made at higher frequencies, it is known that the structure at a given epoch can be attributed primarily to a few distinct features (these are mostly

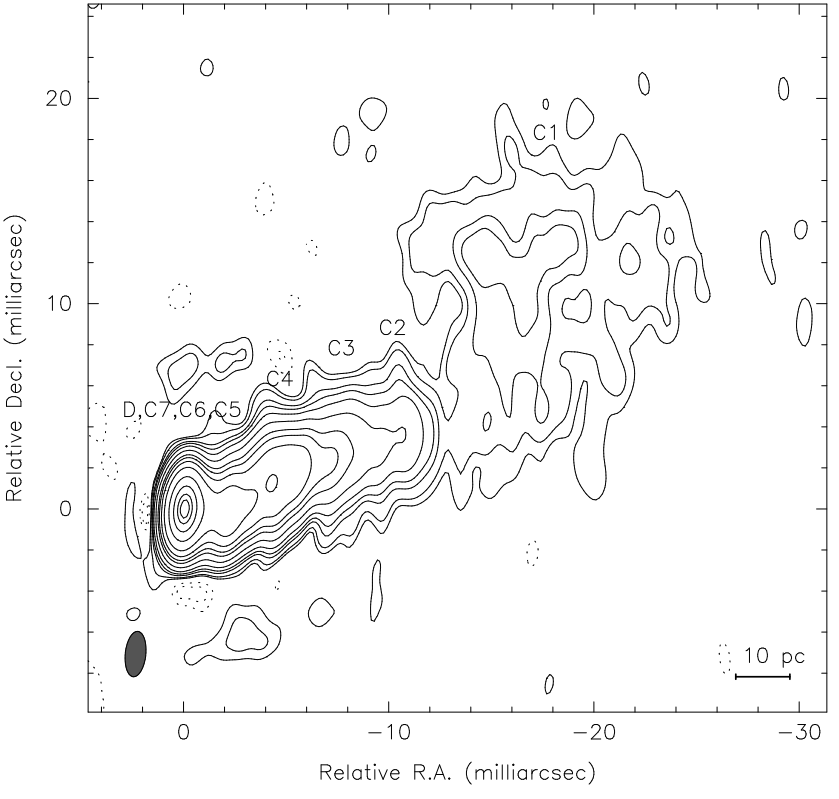

Figure 2 The parsec-scale jet of 3C 345 at 5 GHz, June 1992 (from JA Zensus, AP Lobanov, KJ Leppänen, SC Unwin, and AE Wehrle, in preparation. Contours are −0.1, −0.06, 0.06, 0.1, 0.2, 0.3, 0.5, 1, 2, 3, 5, 10, 25, 50, 75, and 90% of the peak, 3.17 Jy per beam. The restoring beam is 2.22 × 1.0 milliarcsec, at PA −6°.

blended in the image shown). These features typically have been tracked for several years. In 3C 345, for example, high-dynamic range work has revealed a complex filamentary underlying jet flow (Unwin & Wehrle 1992).

An increasing number of core-dominated quasars like 3C 345 have been imaged in fascinating detail; two other examples are 3C 273 (Zensus et al 1990, Davis et al 1991, Unwin et al 1994a, Bahcall et al 1995) and 0836+710 (Hummel et al 1992a). The 18-cm image of 3C 273 has a dynamic range (defined as the ratio of image peak and lowest believable feature) exceeding 5000:1, and the image traces the jet to more than 150 milliarcsec from the core. An extended secondary feature detected as separate from the arcsecond jet has been speculated to be the elusive counterjet feature (Davis et al 1991). In general, however, no convincing counterjet has been found in any core-dominated, i.e. presumably strongly boosted, source. The 2000:1 dynamic range image of 0836+710 was made by combining VLBI data with VLBA and MERLIN observations and traces the complex continuous jet in this source from parsec to kiloparsec scales (Hummel et al 1992a).

These examples demonstrate a significant trend: Images of luminous sources typically show continuous jets with rich substructures, which are markedly different from the simple structures represented in maps from only a few years ago. In some cases, the jets are resolved in transverse directions, and filaments, limb-brightening, and edge-brightening have been reported. The technical advance in imaging capability has brought with it the need for more complicated models to explain the properties of the sources under study. The main features in these images still correspond to the "distinct components" seen in older maps, but state-of-the-art images tend to reveal weaker features and often directly reveal the underlying continuous jet emission. The evidence for the apparent superluminal motions in the best-studied sources has remained strong, but at the same time it is clear that infrequent sampling in time is bound to cause misidentification and confusion. Any motion is typically not uniform, and several values of motion have been observed in a given source. In particular, there coexist in some cases slow or stationary features and fast-moving regions. Little is known about the kinematic properties of the underlying continuous jet component. Although subluminal motions have been observed mostly in radio galaxies (e.g. Cygnus A, M 87, 3C 84, Centaurus A), there are some quasars with subluminal components as well (e.g. 0153+74).

There are a number of highly compact sources that show intraday variability (see Wagner & Witzel 1995). Although refractive interstellar scintillation can explain so far only the lower-frequency behavior in cases like 0917+624, it must have some effect in all very compact objects (Rickett et al 1995); the correlated variability between radio and optical and between optical and X rays, such

as those found in 0716+714 (Wagner et al 1996), probably rules out a solely extrinsic origin (Qian et al 1995).

FR II Radio Galaxies and Quasars

Relativistic beaming models attribute the diversity in properties of extragalactic radio sources to orientation effects (e.g. Scheuer & Readhead 1979, Blandford & Königl 1979, Orr & Browne 1982, Barthel 1989). The cores of extended radio galaxies and quasars tend to be much weaker and presumably are not strongly relativistically beamed towards us. The systematic study of morphology and parsec-scale jet velocities offers the opportunity to test the beaming hypothesis by measuring the distribution of parsec-scale jet speeds. This requires selection of samples with minimal orientation bias, e.g. samples of lobe-dominated quasars from low-frequency surveys. So far, there is an intriguing trend that the observed speeds (in eight cases to date) are in the range $v_{\rm app} \sim 1$–$5\ h^{-1}c$ (Hough et al 1996a, Hough 1994, Hough & Readhead 1989, Vermeulen et al 1993, Porcas 1987, Zensus & Porcas 1987). The quasar 3C 263 is fascinating; this source shows a one-sided core-jet morphology similar to that of core-dominated sources like 3C 345, with evidence for mild acceleration and nonradial motion of jet components (Hough et al 1996). So far, the relatively low superluminal speeds, together with these properties in 3C 263, tentatively support the unification of core- and lobe-dominated quasars.

Cygnus A (3C 405) is the closest luminous radio galaxy (see Carilli & Barthel 1996, Carilli & Harris 1996, and references therein). It is presumably oriented at a large angle ($>60^\circ$) to the line of sight and presents the best-studied case of a parsec-scale jet in a FR II radio galaxy (Carilli et al 1994, 1996, Bartel et al 1995, Krichbaum et al 1996, 1997). The parsec structure contains a knotty jet and a weak counterjet. The jet extends to about $300\ h^{-1}$ pc from the core (at 1.6 GHz), it is well collimated, and it contains subluminal component motion, measured at 5 GHz in the range 0.35–0.55 $h^{-1}c$. There is no emission gap between jet and counterjet observed, in contrast to some inner-jet model predictions (Marscher 1996).

Close to the radio core of Cygnus A (Figure 3), the observed speed is even lower (0.1–0.2 $h^{-1}c$), which indicates the presence of acceleration or pattern speeds (Krichbaum et al 1997). Oscillations of the jet ridge line and jet width may reflect jet instabilities (e.g. Kelvin-Helmholtz), which in turn would predict a pattern speed slower than the fluid speed (Hardee et al 1995). Assuming intrinsic symmetry, the frequency-dependent jet-to-counterjet ratio can be explained by partial obscuration of the counterjet, perhaps by a disc or torus (see Carilli & Barthel 1996). Overall, the properties of Cygnus A jet are compatible with the simple relativistic beaming model; the speed of the jet fluid at larger

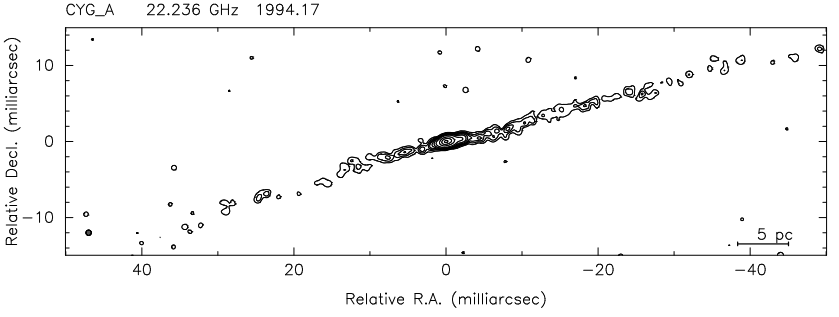

Figure 3 The inner jet and counterjet of Cygnus A at 22 GHz, at epoch 1994.17 (from Krichbaum et al 1997). The field of view is $\sim$100 $\times$ 30 milliarcsec. The size of the circular beam is 0.7-mas size and the contour levels are -0.05, 0.05, 0.15, 0.3, 0.5, 1, 2, 5, 20, 50, and 90% of the peak flux density of 0.73 Jy/beam. The total flux density of the map is 1.65 ± 0.05 Jy.

core-distances is $0.4 \lesssim \beta \lesssim 0.6$ and the inclination is $35^\circ \lesssim \theta \lesssim 90^\circ$ (Bartel et al 1995). However, given the slow apparent speed, the unification of Cygnus A type objects with blazars is difficult unless the intrinsic-jet Lorentz factor in this source is similar to that of quasars (Krichbaum et al 1997).

FR I Radio Galaxies and Quasars

Systematic VLBI studies of FR I radio galaxy samples indicate that they are similar in morphology to FR II cores (Giovannini et al 1995, Pearson 1996): Asymmetric core-jet structures are typical (e.g. 3C 465, Venturi et al 1995) although in a few cases two-sided jets (e.g. 3C 338, Feretti et al 1993) or complex structures are found (e.g. 3C 272.1, Giovannini et al 1995). Jets tend to be well collimated close to the respective nucleus, they lie almost always on the same side as the larger-scale jets, and a higher degree of asymmetry seems to exist on small angular scales as compared with large angular scales. Stationary components are observed, as well as subluminal and slow superluminal motion (0.5–$1.2\,h^{-1}\,c$), which indicate that these jets are indeed relativistic. On the hypothesis that the radio structures are affected by Doppler favoritism, jet velocity and inclination to the line of sight can be derived from jet-to-counterjet ratios, from the ratio of core and total radio power, from Inverse-Compton arguments, and from imposing an upper limit to the deprojected size of a given source. Lorentz factors $\gamma \sim 3$ and viewing angles larger than 30° have been derived that are consistent with unification of low- and high-power radio galaxies (Giovannini et al 1994, 1995).

The best-studied objects in this category are the two nearby objects M 87 and Centaurus A. The radio galaxy M 87 (3C 274) contains the nearest powerful extragalactic jet in the northern hemisphere (Biretta 1996, Biretta & Junor 1995,

and references therein) and offers unique opportunity for detailed study. This one-sided jet is characterized by filamentary features, limb-brightening, and side-to-side oscillations. The innermost part of the jet within 10^{16} cm from the center is well collimated and slightly curved (Junor & Biretta 1995). Prominent features on parsec and subparsec scales are stationary; at larger distances there is subluminal motion of $\beta_{\rm app} = 0.28 \pm 0.08$ (Reid et al 1989); and on a kiloparsec scale, apparent superluminal motion is evidenced up to $\beta_{\rm app} \approx 2.5$ (Biretta et al 1995). Together with the absence of a visible counterjet, these results are consistent with an underlying relativistic jet flow of Lorentz factor γ of about 2 and initial collimation at distances less than $0.1\ h^{-1}$ pc from a suspected black hole/accretion disk at the center (Biretta & Junor 1995).

The giant radio galaxy Centaurus A (NGC 5128) is the closest radio galaxy and contains a straight jet of about 50 milliarcsec in extent in the same direction as the arcsecond and X-ray jet in the source (Tingay et al 1994, Jauncey et al 1995). The source varies rapidly on time scales shorter than four months and shows subluminal motion of about $0.15\,h^{-1}\,c$. The low speed and evidence for a subparsec-scale counterjet suggest that this jet is nonrelativistic or only mildly relativistic, that it is oriented at a large inclination, and that the innermost 0.4–0.8 h^{-1} pc of the source is seen through a disk or torus of ionized gas that is opaque at lower frequencies owing to free-free absorption (Jones et al 1996).

The size of the compact radio nucleus of Centaurus A is 0.5 ± 0.1 milliarcsec (Kellermann et al 1997). The corresponding linear dimensions of 0.01 pc, about 10 light-days or 10^{16} cm, make this the smallest known extragalactic radio source. If the radio lobes are powered by a massive central engine, such as a black hole, their large total energy contents suggest that the central mass density may have exceeded 5×10^{13} $M_\odot$ pc^{-3}, a value far larger than has been determined for any other AGN or quasar.

Two other prominent objects in this class are NGC 6251 (Jones & Wehrle 1994) and the core-dominated superluminal galaxy 3C 120, where the jet has been traced for about 500 milliarcsec from the core (Walker et al 1987, Benson et al 1988, RC Walker & JM Benson, personal communication).

A special case of a core-dominated source with FR I type radio morphology is 3C 84 (Figure 4), associated with the prominent Perseus cluster galaxy NGC 1275. On parsec scales, the source contains a broad complex jet with several components that exhibit subluminal motion of about $0.1\ h^{-1}c$ near the core and $0.5\,h^{-1}c$ at larger distances (see Romney et al 1995 and references therein; see also Venturi et al 1993, Krichbaum et al 1993b). A weak counter feature with strong low-frequency cutoff is found (Vermeulen et al 1994, Walker et al 1994); because of its low surface brightness, this cannot be explained by synchrotron self-absorption. Levinson et al (1995) have instead proposed obscuration through free-free absorption of the counterjet (but not the jet) by a

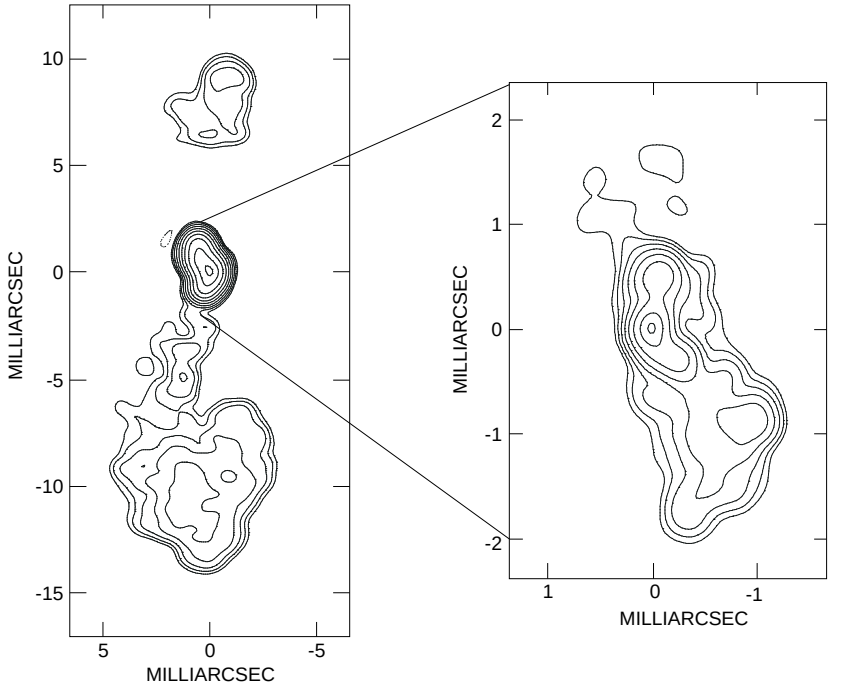

Figure 4 VLBA images 3C 84 at 15 and 43 GHz (from Dhawan, Kellermann, & Romney, in preparation). (*left*): 15 GHz; contours are drawn at −0.25, 0.25, 0.5, 1, 2, 4, 8, 16, 32, 64, and 95% of the peak, 3.49 Jy/beam. (*right*): 43 GHz; contours are drawn at −1, 1, 2, 4, 8, 16, 32, 64, and 95% of the peak, 0.75 Jy/beam.

torus or disk region ionized by the central continuum source. This raises concern about the validity of jet-counterjet ratio arguments made in explanation of source properties by beaming, although Walker et al (1994) conclude that the obscuring region is probably irrelevant at high frequencies and that many properties including the motion in this source are consistent with a mildly relativistic symmetric twin jet at modest inclination. The nucleus in 3C 84 shows radio emission out to a total length of 0.1 arcsec (24 h^{-1} pc), which indicates activity of the central engine for centuries preceding the last outburst observed in 1960 (Taylor & Vermeulen 1996).

Compact Steep Spectrum Sources and Compact Symmetric Objects

On the order of 20–30% of compact sources in flux-density–limited surveys at lower frequencies (e.g. 3CR) belong to the compact steep spectrum (CSS) class

(Fanti et al 1990). These galaxies or quasars are typically small (<2 arcsec or linear sizes $\leq$10–15 h^{-1} kpc) and exhibit a steep radio spectrum ($\alpha > -0.5$); few have been found to show evidence for the presence of relativistic components. The giga-Hertz–peaked spectrum sources (O'Dea et al 1991, O'Dea 1996), subkiloparsec-size objects with radio spectra that peak at giga-Hertz frequencies, are considered part of this class.

In a morphologic sense, three subgroups have been identified: compact symmetric objects (CSO, size $<0.5\ h^{-1}$ kpc), medium-size symmetric objects (MSO, size ≥ 0.5 kpc), and complex sources (Readhead 1995, Fanti & Spencer 1996). The latter are mostly identified as quasars with core-jet structures where the jets dominate (Spencer 1994).

The distortions in the sources with complex structures have been attributed to beaming and/or "frustration" by interaction with a dense interstellar medium (Spencer 1994) that would inhibit the growth of the structures to large dimensions. Figure 5 shows VLBI polarization images of the superluminal CSS quasar 3C 138 (Cotton et al 1997). The magnetic field in this complex jet is aligned

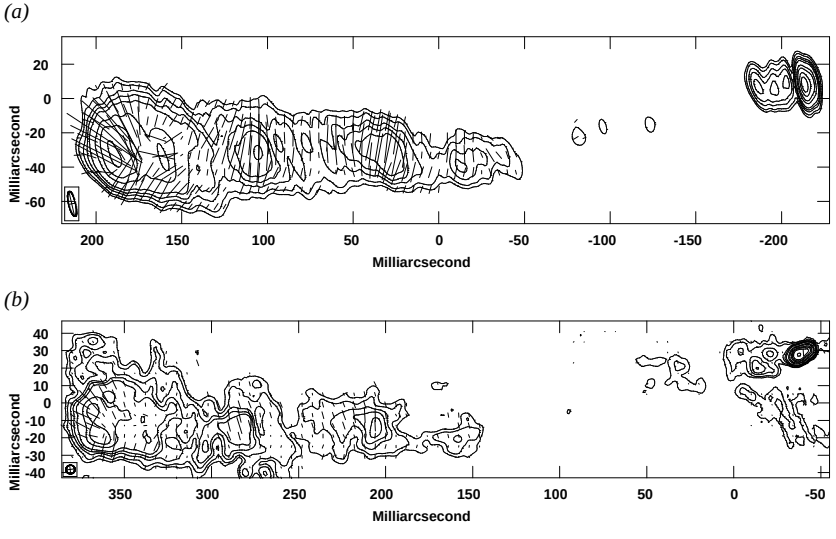

Figure 5 The core and jet in the CSS quasar 3C 138 (from Cotton et al 1997). (*a*) Image at 18 cm, made with the EVN and the VLBA. The peak in the image is 241 mJy/beam and contours are drawn at -5, 5, 8, 14, 19, 27, 54, 81, 135, 189, and 270 mJy/beam. The lengths of the polarization vectors are proportional to the polarized intensity and have the orientation of the electric field vectors. (*b*) Image at 5 GHz, made with the VLBA. The resolution is 5 milliarcsec and the beam is shown in the lower left corner. The peak in the image is 215 mJy/beam and contours are drawn at -2, 2, 3, 5, 7, 10, 20, 30, 50, 70, 100, and 200 mJy/beam. Vectors as in *a*. Note that total intensity images of this source also show a weak feature on the opposite side from the jet.

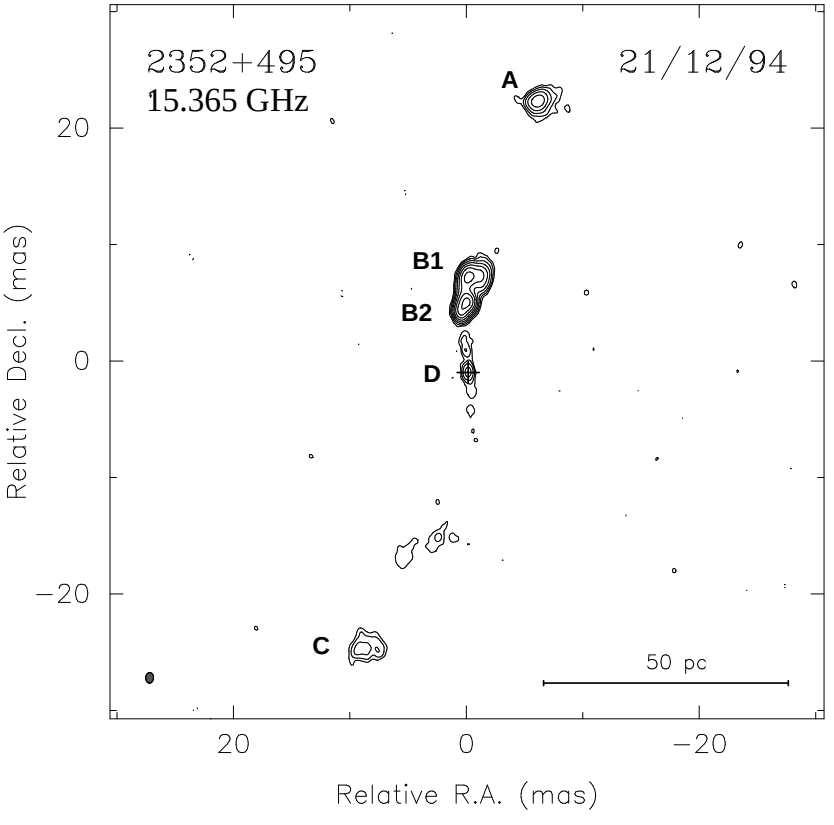

Figure 6 A 15-GHz VLBA image of the CSS source 2352+495 (from Taylor et al 1996). Contours are drawn at −0.75, 0.75, 1.5, 3, 6, 12, 24, 48, 96 mJy/beam, and the beam is 0.91 × 0.67 milliarcsec. Component D is identified with the core, and A and C with hot spots.

along the jet axis and wraps around the head of the jet. The nuclear region is depolarized at 1.7 GHz, and there is no evidence for significant magnetized plasma in front of the end of the jet. At least in this case, the data suggest that this is not a jet that is frustrated by a dense interstellar medium.

The CSO sources comprise 5–10% of all high-luminosity AGN and are probably related to the "compact double" type (Phillips & Mutel 1982). Figure 6 shows an example, 2352+495 (Taylor et al 1996). The identification of the center of activity in this and other CSOs is often difficult due to low core fractions and complex structures. Most objects in this class are identified with galaxies (but see Perlman et al (1994) for a possible BL Lac object with CSO properties

and a parsec-scale counterjet). Typically the CSOs show a very weak core, two symmetric lobes or hot spots, and resolved jet-like emission on one side. The ratio of jet length to counterjet length is close to unity, and higher pressure and smaller hot spots are seen on the jet side. It is still unclear if this asymmetry is intrinsic or instead caused by beaming and/or environmental effects. Within a simple unification model of radio sources, the CSOs and MSOs appear likely to be young and intermediate progenitors of large-scale FR II objects that show decreasing luminosity as they expand (Readhead et al 1996a,b, Fanti et al 1995).

STRUCTURAL VARIATIONS

Apparent Superluminal Motion

Statistical results from the study of motions in large samples of superluminal sources have been discussed by Ghisellini et al (1993), and Vermeulen & Cohen (1994), and Vermeulen (1995), for example. These studies aim at developing population models that test for the presence of a distribution in lieu of a constant value of Lorentz factor, pattern speeds that differ from fluid speeds, jet bending, and accelerations. For a sample of 81 flat-spectrum objects, Vermeulen (1995) found no evidence for intrinsically different populations of galaxies, BL Lac objects, and quasars, which is in contrast to other reports (see Gabuzda 1995). Apparent velocities $\beta_{\rm app}$ in the range 1–5 $h^{-1}c$ occur with roughly equal frequency (Figure 7), and in particular, higher values up to $\beta_{\rm app} = 10\,h^{-1}$ are rarer than assumed from earlier studies of superluminal sources (see Figure 7). This velocity distribution can be reproduced by assuming a wide range of Lorentz factors. Finally, a rising upper envelope to the $\beta_{\rm app}$ distribution appears to exist when plotted as a function of 5-GHz luminosity. This is consistent with the high-luminosity sources in the sample existing as strongly Doppler-beamed members of a parent population with much lower intrinsic luminosity.

In the majority of cases, the evidence for apparent superluminal motion is based on few observations, and accordingly, such statistical studies usually assume that the motion measured for a particular superluminal source component is along ballistic trajectories at constant speed. Detailed monitoring studies have shown that in a given source, not only can different components have different speeds, but accelerations and decelerations are present in several sources. Stationary features have been observed in a few instances. In addition, rarely are the reported motions along straight ballistic trajectories: Kinks and bends are frequently seen, and in a small number of cases, complicated curved trajectories have been determined. Note that such curvature sometimes is measured not directly for a given component, but indirectly by tracing several components, e.g. along a jet that might be characterized by a well-defined ridge line

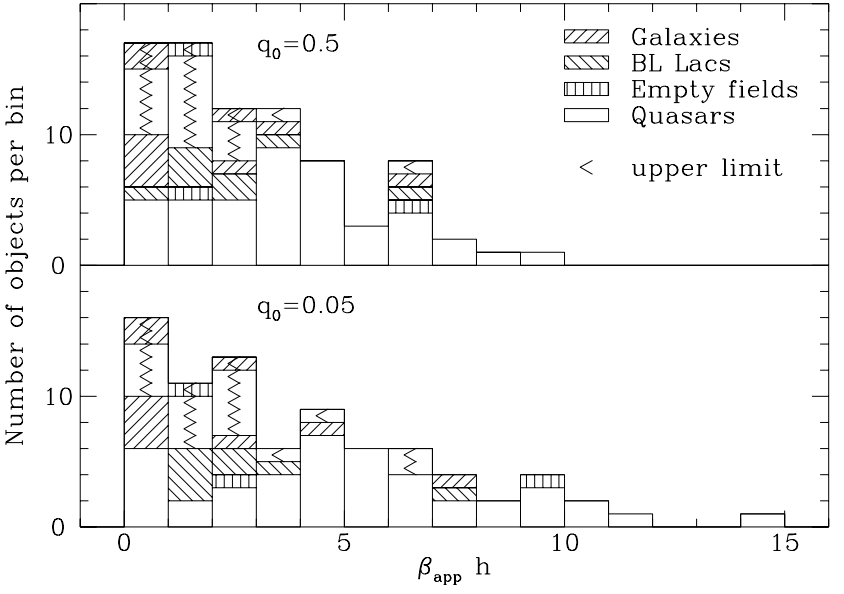

Figure 7 The observed apparent velocity distribution for 81 objects in a homogeneous flat-spectrum sample is illustrated, showing that higher values are rare, compared with earlier work and predictions for beamed samples (from Vermeulen 1995).

or time-averaged mean jet axis. The curvature and nonlinear motion along bent trajectories that is seen so often is perhaps the strongest evidence against the existence of truly moving plasmons as the physical nature of superluminally moving components.

Curved Trajectories

Figure 8 shows the different apparent trajectories (in the region 1 milliarcsec from the core) of the superluminal features of 3C 345 (JA Zensus, AP Lobanov, KJ Leppänen, SC Unwin, and AE Wehrle, in preparation), as measured with respect to the stationary core D (Bartel et al 1986). These tracks are substantially curved and show kinks and bends. Note that at larger distances from the core, the components appear to roughly follow the same curved trajectory in the northwest direction towards the arcsecond structure; near the core the trajectories differ significantly. Note that in this and other sources, the curvature appears most pronounced near the core—reflected in bends and wiggles with amplitudes of <0.2–0.5 milliarcsec. There should also be opacity effects causing frequency dependency of component shapes and positions and of the

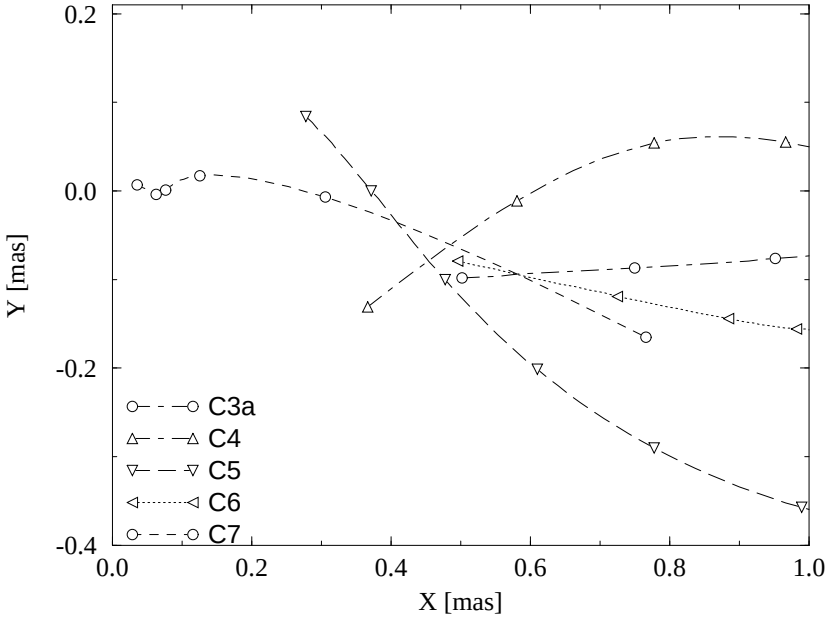

Figure 8 The trajectories of superluminal features in 3C 345 within 1 milliarcsec from the core are shown (JA Zensus, AP Lobanov, KJ Leppänen, SC Unwin, and AE Wehrle, in preparation), measured with respect to the core D. Lines are from polynomial fits to x and y coordinates in time.

observed trajectories. Such behavior is seen, for example, in 3C 345 and also in 4C 39.25 (Alberdi et al 1997).

Similar curved trajectories or jet ridge lines have been reported in a growing number of cases, especially from high-resolution observations at millimeter wavelengths (Krichbaum et al 1994b, Bååth 1994, Krichbaum et al 1994a). The BL Lac object 1803+784 shows quasisinusoidal curvature in a parsec-scale jet (Krichbaum et al 1994b). The extrema in apparent velocity occur at or near the turning points in the curvature.

IIK Pauliny-Toth (personal communication) finds from observations during 1983–1990 that the jet in the quasar 3C 454.3 is curved, which is confirmed by observations at 3 mm (Krichbaum et al 1995). A correlation between curvature and velocity changes is also observed in 3C 84 (Krichbaum et al 1993a,c) at high frequencies, with components accelerating from <0.1 to $\sim 0.5\ h^{-1}\ c$ (see also Romney et al 1995, Dhawan et al 1997, and references therein). In 3C 273, it is not clear if all components follow the same path,

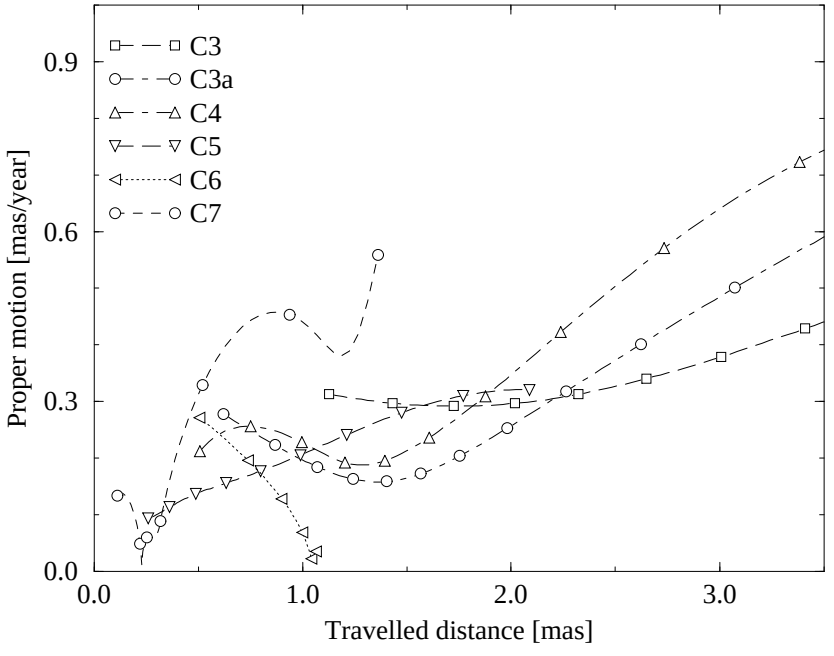

Figure 9 Proper motions in 3C 345 (from JA Zensus, AP Lobanov, KJ Leppänen, SC Unwin, and AE Wehrle, in preparation) are shown, as derived from polynomial fits in relative coordinates x and y (see Figure 8).

although at least two component pairs have indistinguishable trajectories within the bent jet (Krichbaum et al 1993a, Abraham et al 1996).

Variable Component Speeds

Figure 9 shows the apparent angular speed for components in 3C 345 versus distance traveled along the corresponding curved trajectory (JA Zensus, AP Lobanov, KJ Leppänen, SC Unwin, and AE Wehrle, in preparation). The plot highlights the complex nature of the velocity changes that occur in this source. To the first order, the component speeds increase with separation from the core, but there is evidence for a systematic minimum speed at 1–1.5 milliarcsec from the core, which perhaps indicates transition between physically different (the inner and outer) regions of the jet, although a purely geometric explanation is not ruled out. The kinematics and luminosity changes in 3C 345 suggest that the accelerations measured are intrinsic (Qian et al 1996). In the quasar 0836+71, three regions show different apparent speeds. There appears to be a correlation between superluminal speed and jet expansion in this source, i.e. in the narrow region of the jet there is no measured motion, and where the jet opens, speeds

range between 5 and 10 $h^{-1}\,c$, with the faster motion occurring close to the core (Krichbaum et al 1990b).

The quasar 4C 39.25—first thought to be a stationary double source and later thought to be a candidate for superluminal contraction (Shaffer & Marscher 1987)— shows a component moving between two stationary features (Alberdi et al 1993b), not unlike the case of 3C 395 (Simon et al 1988). Recent observations at 22 and 43 GHz demonstrate that the apparent speed slows down as the moving feature approaches the eastern stationary feature (see Alberdi et al 1993a). There is also some evidence that there are apparent differences in the jet curvature in the 22- and 43-GHz images (Alberdi et al 1997). This has been explained in terms of repeated bending of the jet; the stationary features correspond to the Doppler-enhanced underlying jet flow where it is oriented almost along the line of sight (Marcaide et al 1994a). Alternatively, the stationary features have also been explained by standing shocks (Gómez et al 1994, Hughes et al 1989a) and interactions with the narrow line region (Taylor et al 1989); e.g. see the extended component C1 in 3C 345 (Unwin & Wehrle 1992).

Acceleration (and superluminal brightening) have also been found in 3C 454.3 (Pauliny-Toth et al 1987; IIK Pauliny-Toth, personal communication); apparent speeds increase nonlinearly with separation from the core. For separations from the core of 1–2 milliarcsec, the speed is about 8.4 $h^{-1}c$; from 2- to 5-milliarcsec separation, the speed increases continuously to about 21 $h^{-1}\,c$. Beyond that core distance, the speed is uncertain because the components become complex. All this is based on data between 1983 and 1990. The high-redshift blazar 0528+134 ($z = 2.07$) shows three moving features and at least one stationary component. One of these appears to be related to a γ-ray/millimeter flare (Krichbaum et al 1995). In the quasar 1928+738, there appears to be a transition zone at about 4–6 milliarcsec from the core, similar to the case of 3C 345, which separates two jet regions with different apparent component speeds: At separations from the core smaller than 4 milliarcsec, speeds of about 4c were measured (Hummel et al 1992b), whereas between 6 and 18 milliarcsec from the core, the speeds are 6 to 7 $h^{-1}c$ (Schalinski et al 1992). Finally, in 3C 273 there are also different apparent component speeds and again a trend that the speeds are higher at larger distances from the core (Zensus et al 1990, Krichbaum & Witzel 1992, Abraham et al 1996).

In the sources observed with VLBI, there is often assumed to be no difference between pattern and fluid speed. The occurrence of different component speeds, as in M 87 (see Biretta & Junor 1995), 3C 120, or Cygnus A—if not interpreted by geometric effects—might be caused by variable pattern speed (Vermeulen & Cohen 1994). Some theoretical studies predict, for example, interacting instability modes that can produce variable observed pattern speeds (Hardee et al 1995).

Broadband Activity and Emergence of New Jet Components

The study of multiwavelength total flux-density variability offers an important diagnostic in testing models for the "inner jet" in blazars, and it is complementary to direct observation of structural variability (see Marscher & Bloom 1994, Marscher 1995, Marscher 1996). In particular, nonthermal flaring activity from radio to γ-ray frequencies is expected to show frequency-dependent time delays that are model specific. The γ-ray emission detected in a large number of blazars (Von Montigny et al 1995) is most likely to be produced from inverse-Compton scattering from relativistic jet electrons, although the details of this process are not yet clear. Several such blazars are therefore being subjected to multiwavelength monitoring campaigns that are beginning to show model-discriminating results (see Marscher 1996). The superluminal quasar 3C 279 (e.g. Carrara et al 1993) has been intensively monitored over a large spectral range (Maraschi et al 1994, Grandi et al 1996), and there is VLBI component activity near coincident with γ-ray flaring (Wehrle et al 1994a,b). For the blazar PKS 0420−014, helical structure and new component ejection were predicted from simultaneous optical and γ-ray flaring (Wagner et al 1995), and so far VLBI imaging has confirmed curvature in the structure of this source. Several other γ-ray active blazars, including 0528+134, 3C 273, and 0836+710, are also being investigated with VLBI at millimeter wavelengths, and here new features have been observed near γ-ray flares and at the onset of millimeter-flux density activity, which perhaps suggests a causal connection (Krichbaum et al 1995, Britzen et al 1997). A correlation between γ-ray outbursts and superluminal motion might suggest the existence of relativistic γ-ray jets, i.e. within as close as a few light-days to the central engine in such objects. One of several alternative explanations is that the γ-ray bursts might be related to precessing relativistic $e^{\pm}$ beams (Roland et al 1994).

BL Lac is perhaps the best example for a correlation between variability in the centimeter regime and the appearance of superluminal features that can be modeled with shocks (Mutel et al 1990, Mutel et al 1994, Denn & Mutel 1996). In this source, the position angles of the axes of the curved trajectories of subsequent components shift, suggesting evidence for precession caused by a binary black hole system (Mutel et al 1994). Note that such a scenario was also proposed for the superluminal quasar 1928+738 (Hummel et al 1992b, Roos et al 1993).

In 3C 345, several components first appeared following a major flux density increase at centimeter wavelengths, but not all components in this source have been related to such pronounced flux density changes; for example, the recent feature C7 was first seen during a deep minimum in the total flux density. In

this source X-ray variability is correlated to the radio variations supporting the synchrotron self-Compton model for this source (Unwin et al 1997). In 3C 273, a correlation appears to exist between the ejection of superluminal features with flares in the radio and infrared/optical regimes (Krichbaum et al 1990a, Abraham et al 1996). A possible correlation of the speed of a component in this source with the amplitude of a perhaps related optical outburst has been speculated to exist (Bhabadzhanyants & Belokon 1992). In 3C 454.3, a new component appeared around 1983, with an apparent mean motion of 0.81 ± 0.04 mas yr^{-1} ($v/c = 20.4\,h^{-1} \pm 1.0$). Extrapolation gives a time of zero separation of 1982 $\pm$ 3, i.e. close to the time of a radio outburst (Pauliny-Toth et al, in preparation).

PHYSICAL CONDITIONS IN THE PARSEC-SCALE JETS

Despite the observational and theoretical advances in the study of compact radio sources, the physical nature of the VLBI components observed in parsec-scale radio jets and their connection to the central engine remains unclear (e.g. Marscher 1996). Turbulent plasma inhomogeneities and shock waves have been proposed with considerable success in explaining specific source properties (Blandford & Königl 1979, Reynolds 1982). In the relativistic jet model, the optically thick cores in the VLBI images represent the base of the jet (located near the apex of the jet cone), and the superluminal features are regions of enhanced emission moving along the jet. Theoretical predictions of synchrotron self-Compton emission from the VLBI components can be compared with observed X-ray fluxes or limits, and an observed excess of predicted versus observed X rays is once again interpreted as evidence for bulk relativistic motion (see Marscher 1987). The corresponding Doppler factors constrain allowed ranges of model parameters. In a core-jet source, the inhomogeneous jet model for the core (Königl 1981) can be combined with (perhaps simplistic) homogeneous spheres for the moving components to estimate the basic properties of the parsec-scale emission regions and to derive Doppler factors for the relativistic motion (Marscher 1987, Zensus et al 1995).

Ghisellini et al (1993) derive Doppler factors for about 100 sources with known VLBI structures by comparing predicted and observed X-ray flux in the synchrotron self-Compton model. The main results agree with those from other beaming indicators (superluminal motion and core to extended-flux density ratio) and support a simple kinematic model of ballistic motion of knots in relativistic jets. The derived Doppler factors are largest for core-dominated quasars, intermediate for BL Lacertae objects, and smallest for lobe-dominated radio galaxies and quasars. For the subsample of 39 superluminal sources,

apparent expansion speeds and Doppler factors correlate and have similar average numerical values. This is taken as evidence that the bulk motion causing the beaming also causes the superluminal expansion and that it does not require different pattern and bulk velocities. The corresponding Lorentz factors are about 10 on average, with no significant differences between core- and lobe-dominated quasars and BL Lacs. The derived viewing angles differ, with radio galaxies, lobe-dominated quasars, BL Lacertae objects, and core-dominated quasars representing increasingly aligned objects.

In the case of 3C 345, the synchrotron self-Compton model reconciles well the component radio spectra, including the flat radio spectrum of the core, with the observed flux density, spectrum, and correlated variability in the X rays (Zensus et al 1995, Unwin et al 1994, Unwin et al 1997). The best-fit model requires a very small opening angle ($\sim 0.5^\circ$) for the portion of the jet near the apex of the cone that represents the flat-spectrum radio core; the apparent opening angle is much larger owing to projection effects. The inverse Compton calculations suggest that typically the core and its nearest moving component dominate the X-ray emission. The model is consistent with a heavy proton/electron jet that would yield enough power to fuel the outer radio lobe, and it argues for a small angle to the line of sight of about 1°. This can be relaxed if a pattern speed smaller than the true fluid speed is allowed. Combination of the superluminal speed (from VLBI) and the Doppler factor deduced from the synchrotron self-Compton calculation for the more recently ejected component (C7) implies that the jet bends away from the line of sight (from $\theta \simeq 2^\circ$ to $\simeq 10^\circ$), and such combination also implies that it accelerates from $\gamma \simeq 5$ to $\gtrsim 10$ over the range of (deprojected) distance from the nucleus of $\simeq 3$ to $\simeq 20\ h^{-1}$ pc (Unwin et al 1997).

Helical Jets

Superluminal motion requires that the jet must be relativistic and viewed at a narrow angle to the line of sight so that projection effects are likely to be significant. It is possible to reconstruct the three-dimensional trajectory of a moving feature if an assumption is made for the Lorentz factor, γ, of the motion. If, for example, a constant pattern speed is assumed, the motion of the outer components in 3C 345 can be reconciled with one fixed curved trajectory where the apparent acceleration is due to changes in angle to the line of sight (Wardle et al 1994). For component C4, the observed curvature and acceleration, and the modest decline in (Doppler-boosted) flux density, are consistent with a curved jet of constant Lorentz factor of γ about 10 (Zensus et al 1995a). The derived intrinsic jet curvature is small, but it is greatly amplified by projection effects, and the angle of the jet to the line of sight increases smoothly with radius from the core from ~ 1 to $\sim 4^\circ$.

The observed apparently bent jets with components moving on different ballistic trajectories found in a number of sources can be explained by precession in the region of the nucleus (Blandford 1987): for example, caused by gravitational interaction between galaxies, binary black holes, or black-hole/disk systems. However, the required periods are typically short and cannot easily be reconciled with realistic models (Linfield 1981, Roos 1988). On parsec scales, orbital motion may be a better explanation for the origin of the observed jet structure and kinematics (Roos et al 1993).

A number of models have also been proposed based on helical motion of some sort to explain the curved quasiperiodic trajectories seen in 3C 345, 1803+78, 4C39.25, and similar sources (Camenzind & Krockenberger 1992, Hardee 1987, Königl & Choudhuri 1985, Camenzind 1986, Qian et al 1991, 1996). Helical features in jets are also readily explained from three-dimensional Kelvin-Helmholtz jet simulations (Hardee et al 1995). For the case of 3C 345, the basic properties of component trajectories and apparent velocities for components C4 and C5 have been explained by a simple helical jet with a straight jet axis, which is based on the conservation of physical quantities (Steffen et al 1995). No clear case for a common helix for all components in this source could be made, perhaps because effects in addition to the helical motion are at work. Again, orbital motion at the base of the jet may be the natural explanation for the lack of a unique helix describing the kinematics of all components (Qian et al 1993).

Spectral Properties

Until recently, most monitoring studies were confined to images of the total intensity of a given source in one or more particular observing bands. This suffices to determine basic morphology and component kinematics, but it lacks important physical information that can only be obtained from measuring the jet spectra from multifrequency work (e.g. Walker et al 1996) and the magnetic field distributions from polarization imaging (e.g. Roberts et al 1991, Cotton 1993, Leppänen et al 1995, Kemball et al 1996).

For 3C 345, by combining images taken at different frequencies at quasisimultaneous epochs (within about six months from each other), spectral information can be obtained and used to measure the basic parameters of the component synchrotron spectra: the turnover flux density and frequency and the integrated flux in the range 4–25 GHz (Lobanov & Zensus 1997). The observed luminosity variations suggest a variable pattern Lorentz factor in at least one component. The core turnover frequency and integrated flux show significantly weaker variations compared to the moving components, which suggests that the primary emission mechanism in the jet might differ from that of the core (although blending of the core with a new component can confuse

the situation); at least two components, C4 and C5, show a peaked evolution of turnover frequency. Such spectral properties are important for testing the hypothesis that the jet components are caused by relativistic shocks (Rabaça & Zensus 1994, Marscher & Gear 1985, Hughes et al 1989b, Marscher et al 1992, Gómez et al 1993). However, the evidence in favor of the shock model is inconclusive so far. The total flux density variations in some sources have been adequately explained with shocks (Hughes et al 1989b). In 3C 345, strong shocks with a variable Doppler factor may well be the mechanism at work in the jet at least near the core, although at larger distances (>2 milliarcsec), the shock model alone does not suffice to explain the observed properties, e.g. the required intrinsic accelerations and long-component life times (Lobanov & Zensus 1997). Alternative models have been proposed that involve interaction with the ambient plasma (Rose et al 1987), e.g. the two-fluid model (Sol et al 1989, Pelletier & Roland 1990, Pelletier & Sol 1992) or nonsynchrotron emission mechanisms, i.e. bremsstrahlung (Weatherall & Benford 1991). For the scenario of an induced helical geometry of the jet, the two-fluid model predicts jet kinematics and flux density variability of a form not unlike those seen for at least one component (C7) of 3C 345 (Roland et al 1994).

The shock-in-jet hypothesis has been applied with success in a number of other sources. Marcaide et al (1994a) apply a detailed model of shock components moving on twisted trajectories to the quasar 4C39.25. BL Lac is perhaps the best-understood case for the interpretation of VLBI components by shocks (Mutel et al 1990).

Polarization Properties

The initial motivation for the application of shock models to VLBI jets came from the modeling of total flux density variability and polarization behavior in sources with comparatively simple jet structure, e.g. BL Lac and 3C 279 (Hughes et al 1989b). Polarization imaging, especially at high frequencies, i.e. with adequate angular resolution, is a prerequisite to understanding the internal physics of sources with more complex VLBI jets (Roberts et al 1991, Wardle et al 1994, Aller et al 1994). Linear polarization–sensitive VLBI observations of compact sources yield direct information on the structure and order of the underlying magnetic fields, the presence and nature of thermal material, the energy of relativistic electrons, and the geometry of emission on submilliarcsec scales. There is evidence for a difference in the polarization properties of quasars and BL Lac objects, and the latter show significantly lower speeds, which argues for a physical and not merely an orientation difference between the two classes of sources (Roberts et al 1990, Gabuzda et al 1994a,b). Brown et al (1994) and Wardle et al (1994) have studied the polarization structure at 5 GHz of 3C 345 and interpreted their results in terms of a comprehensive shock model.

Leppänen et al (1995) obtained high-resolution polarization images of 3C 345 at 22 GHz with the VLBA. Assuming negligible depolarization in the core, they find the electric field predominantly oriented along the jet, i.e. the magnetic field orientation is perpendicular to the jet, in contrast to the lower frequency results that suggested a parallel magnetic field (Wardle et al 1994). Gabuzda (1995) found similar evidence for a perpendicular magnetic field from imaging 3C 345 at 10.7 GHz. An analysis applying the model of Wardle et al to the 22-GHz and subsequent 43-GHz observations suggests that the shock model remains applicable for the case of a moderately strong shock (KJ Leppänen & JA Zensus, in preparation). The 22-GHz polarized structure of 3C 345 shows two additional important features: a turn in the electric vector position angle and a steep decline to zero of the observed polarized intensity between C8 and C7. Both properties can, within the shock model, be explained by a simple helical motion of the moving feature (Steffen et al 1995). For the quasar 3C454.3, 7-mm VLBA imaging also reveals an electric field configuration that is aligned with the predominant jet orientation but orthogonal between the major components of the compact structure (Kemball et al 1996). In both cases, it is not yet clear if the observed changes depend on the strength of the shock, or if they result from changes in the local magnetic field configuration, a helical jet geometry, or from local differential Faraday rotation.

CONCLUSION

Extensive VLBI monitoring studies at centimeter and millimeter wavelengths, enhanced by spectral and polarization imaging, of representative types of AGN can discriminate detailed physical models. When combined with broadband total flux density and polarization observations, and especially with X-ray and γ-ray data that measure the synchrotron self-Compton radiation component, they can be used to determine the overall physical conditions in parsec-scale radio jets. Here is an excellent opportunity to directly compare theoretical predictions with observational data, despite the complexity and the large number of free parameters of theoretical models. Some of the most intriguing areas where this may soon become feasible include the formation of the jets, possible jet acceleration mechanisms, the nature of any nonrelativistic matter involved (e.g. the ambient medium and thermal outflows), and the influence of the central region on the jet dynamics.

ACKNOWLEDGMENTS

I thank Thomas Krichbaum for extensive discussions and helpful suggestions on the subject of this review. Thanks are also owed to K Kellermann, A Patnaik, and A Witzel for critical comments on the manuscript. I am grateful to B

Cotton, V Dhawan, K Kellermann, T Krichbaum, G Taylor, and R Vermeulen for permission to reproduce material, partly in advance of publication.

Literature Cited

Abraham Z, Cararra EA, Zensus JA, Unwin SC. 1996. *Astron. Astrophys. Suppl.* 115:543–49

Alberdi A, Krichbaum TP, Marcaide JM, Witzel A, Graham DA, et al. 1993a. *Astron. Astrophys.* 271:93–100

Alberdi A, Krichbaum TP, Graham DA, Greve A, Grewing M, et al. 1997. *Astron. Astrophys.* In press

Alberdi A, Marcaide JM, Marscher AP, Zhang YF, Elosegui P, et al. 1993b. *Ap. J.* 402:160–72

Aller HD, Hughes PA, Aller MF. 1994. See Zensus & Kellermann 1994, pp. 223–28

Antonucci RRJ. 1993. *Annu. Rev. Astron. Astrophys.* 31:473–521

Appl S, Sol H, Vicente L. 1996. *Astron. Astrophys.* 310:419–37

Bååth LB. 1994. In *VLBI Technology. Progress and Future Observational Possibilities*, ed. T Sasao, S Manabe, O Kameya, M Inoue, pp. 70–74. Tokyo: Terra Sci.

Bahcall JN, Kirhakos S, Schneider DP, Davis RJ, Muxlow TWB, et al. 1995. *Ap. J. Lett.* 452:L91–L93

Bartel N, Bietenholz MF, Rupen MP. 1995. *Proc. Natl. Acad. Sci. USA* 92:11374–76

Bartel N, Herring TA, Ratner MI, Shapiro II, Corey BE. 1986. *Nature* 319:733–38

Barthel PD. 1989. *Ap. J.* 336:606–11

Barthel PD. 1995. *Highlights Astron.* 10:551–57

Begelman MC. 1995. *Proc. Natl. Acad. Sci. USA* 92:11442–46

Begelman MC, Blandford RD, Rees MJ. 1984. *Rev. Mod. Phys.* 56:255–351

Benson JM, Walker RC, Unwin SC, Muxlow TWB, Wilkinson PN, et al. 1988. *Ap. J.* 334:560–72

Bhabadzhanyants MK, Belokon ET. 1992. See Valtaoja & Valtonen 1992, pp. 384–90

Biretta JA. 1996. See Hardee et al 1996, pp. 187–98

Biretta JA, Junor W. 1995. *Proc. Natl. Acad. Sci. USA* 92:11364–67

Biretta JA, Moore RL, Cohen MH. 1986. *Ap. J.* 308:93–109

Biretta JA, Zhou F, Owen FN. 1995. *Ap. J.* 447:582–96

Blandford RD. 1987. See Zensus & Pearson 1987, pp. 310–27

Blandford RD, Königl A. 1979. *Ap. J.* 232:34–38

Blandford RD, Payne DG. 1982. *MNRAS* 199: 883–903

Blandford RD, Rees MJ. 1974. *MNRAS* 169: 395–415

Bridle AH. 1996. See Hardee et al 1996, pp. 383–94

Bridle AH, Perley RA. 1984. *Annu. Rev. Astron. Astrophys.* 22:319–58

Britzen S, Witzel A, Krichbaum TP. 1997. In *Proceedings of the Heidelberg Workshop on Gamma-Ray Emitting AGNs*, ed. JG Kirk, M Camenzind, C von Montigny, S Wagner, pp. 109–12. Heidelberg: Max-Planck-Inst. Kernphys.

Brown LF, Roberts DH, Wardle JFC. 1994. *Ap. J.* 437:108–21

Burbidge EM, Burbidge G. 1997. *Ap. J.* 477: L13–L15

Camenzind M. 1986. *Astron. Astrophys.* 156:137–51

Camenzind M, Krockenberger M. 1992. *Astron. Astrophys.* 255:59–62

Carilli CL, Bartel N, Diamond P. 1994. *Astron. J.* 108:64–75

Carilli CL, Barthel PD. 1996. *Astron. Astrophys. Rev.* 7:1–54

Carilli CL, Harris DE, eds. 1996. *Cygnus A—Study of a Radio Galaxy.* Cambridge: Cambridge Univ. Press

Carilli CL, Perley RA, Bartel N, Sorathia B. 1996. See Hardee et al 1996, pp. 287–98

Carrara EA, Abraham Z, Unwin SU, Zensus JA. 1993. *Astron. Astrophys.* 279:83–89

Cawthorne TV. 1991. See Hughes 1991, pp. 187–231

Cohen MH, Kellermann KI, eds. 1995. *Quasars and Active Galactic Nuclei: High Resolution Radio Imaging, Proc. Natl. Acad. Sci. USA* 92:11339–450

Conway JE. 1994. See Zensus & Kellermann 1994, pp. 73–78

Conway JE, Murphy DW. 1993. *Ap. J.* 411:89–102

Conway JE, Wrobel JM. 1995. *Ap. J.* 439:98–112

Cotton WD. 1993. *Astron. J.* 106:1241–48

Cotton WD, Dallacasa D, Fanti C, Fanti R, Foley AR, et al. 1997. *Astron. Astrophys.* Submitted

Davis RJ, Booth RS, eds. 1993. *Sub-Arcsecond Radio Astronomy.* Cambridge: Cambridge Univ. Press
Davis RJ, Unwin SC, Muxlow TWB. 1991. *Nature* 354:374–76
Denn G, Mutel R. 1996. See Ekers et al 1996, pp. 41–42
Ekers R, Fanti C, Padrielli L, eds. 1996. *IAU Symp. 175: Extragalactic Radio Sources.* Dordrecht: Kluwer
Fanaroff BL, Riley JM. 1974. *MNRAS* 167:31P–35P
Fanti C, Fanti R, Dallacasa D, Schilizzi RT, Spencer RE, Stanghellini C. 1995. *Astron. Astrophys.* 302:317–26
Fanti R, Fanti C, Schilizzi RT, Spencer RE, Nan Rendong, Parma P, et al. 1990. *Astron. Astrophys.* 231:333–46
Fanti R, Spencer R. 1996. See Ekers et al 1996, pp. 63–66
Feretti L, Comoretto G, Giovannini G, Venturi T, Wehrle AE. 1993. *Ap. J.* 408:446–51
Gabuzda DC. 1995. *Proc. Natl. Acad. Sci. USA* 92:11393–98
Gabuzda DC, Cawthorne TV, Roberts DH, Wardle JFC. 1992. *Ap. J.* 388:40–54
Gabuzda DC, Mullan CM, Cawthorne TV, Wardle JFC, Roberts DH. 1994. *Ap. J.* 435:140–61
Ghisellini G, Padovani P, Celotti A, Maraschi L. 1993. *Ap. J.* 407:65–82
Giovannini G, Cotton WD, Feretti L, Lara L, Venturi T, Marcaide JM. 1995. *Proc. Natl. Acad. Sci. USA* 92:11356–59
Giovannini G, Feretti L, Venturi T, Lara L, Marcaide J, et al. 1994. *Ap. J.* 435:116–27
Gómez JL, Alberdi A, Marcaide JM. 1993. *Astron. Astrophys.* 275:55–68
Gómez JL, Alberdi A, Marcaide JM. 1994. *Astron. Astrophys.* 284:51–64
Gopal-Krishna. 1995. *Proc. Natl. Acad. Sci. USA* 92:11399–406
Grandi P, Urry CM, Maraschi L, Wehrle AE, Madejski GM, et al. 1996. *Ap. J.* 459:73–81
Guirado JC, Marcaide JM, Alberdi E, El'osegui P, Ratner MI, et al. 1995. *Astron. J.* 110:2586–96
Gurvits LI. 1994. *Ap. J.* 425:442–49
Hardee PE. 1987. *Ap. J.* 318:78–92
Hardee PE, Bridle AH, Zensus JA, eds. 1996. *Energy Transport in Radio Galaxies and Quasars.* San Francisco: Astronomical Society of the Pacific
Hardee PE, Clarke DA, Howell DA. 1995. *Ap. J.* 441:644–64
Henstock DR, Browne IWA, Wilkinson PN, Taylor GB, Vermeulen RC, et al. 1995. *Ap. J. Suppl.* 100:1–36
Hewitt JN. 1995. *Proc. Natl. Acad. Sci. USA* 92:11434–38
Hirabayashi H. 1996. See Ekers et al 1996, pp. 529–30
Hough DH. 1994. See Zensus & Kellermann 1994, pp. 169–74
Hough DH, Readhead ACS. 1989. *Astron. J.* 98:1208–25
Hough DH, Vermeulen RC, Wood DAJ, Standifird JD, Cross LL. 1996a. *Ap. J.* 459:64–72
Hough DH, Zensus JA, Porcas RW. 1996b. *Ap. J.* 464:715–23
Hughes PA, ed. 1991. *Beams and Jets in Astrophysics.* Cambridge: Cambridge Univ. Press
Hughes PA, Aller HD, Aller MF. 1989a. *Ap. J.* 341:54–67
Hughes PA, Aller HD, Aller MF. 1989b. *Ap. J.* 341:68–79
Hughes PA, Miller L. 1991. See Hughes 1991, pp. 1–51
Hummel CA, Muxlow TWB, Krichbaum TP, Quirrenbach A, Schalinski CJ, et al. 1992a. *Astron. Astrophys.* 266:93–100
Hummel CA, Schalinski CJ, Krichbaum TP, Rioja MJ, Quirrenbach A, et al. 1992b. *Astron. Astrophys.* 257:489–500
Jauncey DL, Tingay SJ, Preston RA, Reynolds JE, Lovell JEJ, et al. 1995. *Proc. Natl. Acad. Sci. USA* 92:11368–70
Jones DL, Tingay SJ, Murphy DW, Meier DL, Jauncey DL, et al. 1996. *Ap. J.* 466:L63–L65
Jones DL, Wehrle AE. 1994. *Ap. J.* 427:221–26
Junor W, Biretta JA. 1995. *Astron. J.* 109:500–6
Kellermann KI. 1993. *Nature* 361:134–36
Kellermann KI, Pauliny-Toth IIK. 1981. *Annu. Rev. Astron. Astrophys.* 19:373–410
Kellermann KI, Zensus JA, Cohen MH. 1997. *Ap. J. Lett.* 475:L93–L95
Kemball AJ, Diamond PJ, Pauliny-Toth IIK. 1996. *Ap. J.* 464:L55–L58
Königl A. 1981. *Ap. J.* 243:700–9
Königl A, Choudhuri AR. 1985. *Ap. J.* 289:173–87
Krichbaum TP, Alef W, Witzel A. 1996. See Carilli & Harris 1996, pp. 92–97
Krichbaum TP, Alef W, Witzel A, Zensus JA. 1997. *Astron. Astrophys.* Submitted
Krichbaum TP, Booth RS, Kus AJ, Rönnäng BO, Witzel A, et al. 1990a. *Astron. Astrophys.* 237:3–11
Krichbaum TP, Britzen S, Standke KJ, Witzel A, Schalinski CJ, Zensus JA. 1995. *Proc. Natl. Acad. Sci. USA* 92:11377–80
Krichbaum TP, Hummel CA, Quirrenbach A, Schalinski CJ, Witzel A, et al. 1990b. *Astron. Astrophys.* 230:271–83
Krichbaum TP, Standke KJ, Witzel A, Schalinski CJ, Grewing M, et al. 1994a. In *Proc. 2nd EVN/JIVE Symp.*, ed. AJ Kus et al, pp. 47–54. Torun: Torun Radio Astronomy Observatory
Krichbaum TP, Witzel A. 1992. See Valtaoja & Valtonen 1992, pp. 205–20
Krichbaum TP, Witzel A, Graham DA. 1993a.

In *Jets in Extragalactic Radio Sources*, ed. HJ Röser, K Meisenheimer, Number 421 in Lecture Notes in Physics, pp. 71–78. Berlin: Springer
Krichbaum TP, Witzel A, Graham DA, Schalinski CJ, Zensus JA. 1993b. See Davis & Booth 1993, pp. 181–83
Krichbaum TP, Witzel A, Graham DA, Standke K, Schwartz R, et al. 1993c. *Astron. Astrophys.* 275:375–89
Krichbaum TP, Witzel A, Standke KJ, Graham DA, Schalinski CJ, Zensus JA. 1994b. See Zensus & Kellermann 1994, pp. 39–44
Leppänen KJ, Zensus JA, Diamond PD. 1995. *Astron. J.* 110:2479–92
Levinson A, Laor A, Vermeulen RC. 1995. *Ap. J.* 448:589–99
Linfield R. 1981. *Ap. J.* 250:464–68
Lobanov AP, Zensus JA. 1997. *Ap. J.* Submitted
Maraschi L, Grandi P, Urry CM, Wehrle AE, Madejski GM, et al. 1994. *Ap. J. Lett.* 435:L91–L95
Marcaide JM, Alberdi A, Gómez JL, Guirado JC, Marscher AP, Zhang YF. 1994a. See Zensus & Kellermann 1994, pp. 141–48
Marcaide JM, Elosequi P, Shapiro II. 1994b. *Astron. J.* 108:368–73
Marscher A, Bloom SD. 1994. pp. 572–81. New York: Am. Inst. Phys.
Marscher AP. 1987. See Zensus & Pearson 1987, pp. 280–300
Marscher AP. 1990. See Zensus & Pearson 1990, pp. 236–49
Marscher AP. 1995. *Proc. Natl. Acad. Sci. USA* 92:11439–41
Marscher AP. 1996. See Hardee et al 1996, pp. 45–54
Marscher AP, Gear WK. 1985. *Ap. J.* 298:114–27
Marscher AP, Gear WK, Travis JP. 1992. See Valtaoja & Valtonen 1992, pp. 85–101
Miller JS. 1995. *Proc. Natl. Acad. Sci. USA* 92:11422–26
Miyoshi M, Moran J, Herrnstein J, Greenhill L, Nakai N, et al. 1995. *Nature* 373:127–29
Moran J, Greenhill L, Herrnstein J, Diamond P, Miyoshi M, et al. 1995. *Proc. Natl. Acad. Sci. USA* 92:11427–33
Mutel RL, Denn GR, Dryer MJ. 1994. See Zensus & Kellermann 1994, pp. 191–96
Mutel RL, Phillips RB, Su B, Bucciferro RR. 1990. *Ap. J.* 352:81–95
Napier PJ, Bagri DS, Clark BG, Rogers AEE, Romney JD, et al. 1994. *IEEE Proc.* 82:658–72
Norman ML. 1996. See Hardee et al 1996, pp. 319–26
O'Dea CP. 1996. See Hardee et al 1996, pp. 85–90
O'Dea CP, Barvainis R, Challis PM. 1988. *Astron. J.* 96:435–54
O'Dea CP, Baum SA, Stanghellini C. 1991. *Ap. J.* 380:66–77
Orr MJL, Browne IWA. 1982. *MNRAS* 200:1067–80
Pearson TJ. 1996. See Hardee et al 1996, pp. 97–108
Pearson TJ, Readhead ACS. 1988. *Ap. J.* 328:114–42
Pelletier G, Roland J. 1990. See Zensus & Pearson 1990, pp. 323–32
Pelletier G, Sol H. 1992. *MNRAS* 254:635–46
Perlman ES, Stocke JT, Shaffer DB, Carilli CL, Ma CP. 1994. *Ap. J. Lett.* 424:L69–L72
Phillips RB, Mutel RL. 1982. *Astron. Astrophys.* 106:21–24
Polatidis AG, Wilkinson PN, Xu W, Readhead ACS, Pearson TJ, et al. 1995. *Ap. J. Suppl.* 98:1–32
Porcas RW. 1987. See Zensus & Pearson 1987, pp. 12–25
Qian S, Witzel A, Krichbaum TP, Wagner SJ. 1995. *Acta Astron. Sinica* 36:34–46. *Transl. Chin. Astron. Astrophys.* 19:522
Qian SJ, Krichbaum TP, Witzel A, Quirrenbach A, Hummel CA, Zensus JA. 1991. *Acta Astro. Sinica* 32(4):369–79. *Transl. Chin. Astron. Astrophys.* 16:137–47
Qian SJ, Krichbaum TP, Zensus JA, Steffen W, Witzel A. 1996. *Astron. Astrophys.* 308:395–402
Qian SJ, Witzel A, Krichbaum TP, Quirrenbach A, Zensus JA. 1993. *Chin. Astron. Astrophys.* 17:150–60
Rabaça CR, Zensus JA. 1994. See Zensus & Kellermann 1994, pp. 163–68
Rantakyrö FT, Bååth LB, Matveenko L. 1995. *Astron. Astrophys.* 293:44–55
Readhead ACS. 1993. See Davis & Booth 1993, pp. 173–80
Readhead ACS. 1995. *Proc. Natl. Acad. Sci. USA* 92:11447–50
Readhead ACS, Taylor GB, Pearson TJ, Wilkinson PN. 1996a. *Ap. J.* 460:634–43
Readhead ACS, Taylor GB, Xu W, Pearson TJ, Wilkinson PN, Polatidis AG. 1996b. *Ap. J.* 460:612–33
Rees MJ. 1966. *Nature* 211:468
Rees MJ. 1971. *Nature* 229:312–17
Reid MJ, Biretta JA, Junor W, Muxlow TWB, Spencer RE. 1989. *Ap. J.* 336:112–20
Reynolds SP. 1982. *Ap. J.* 256:13–27
Rickett BJ, Quirrenbach A, Wegner R, Krichbaum TK, Witzel A. 1995. *Astron. Astrophys.* 293:479–92
Roberts DH, Brown LF, Wardle JFC. 1991. In *Radio Interferometry: Theory, Techniques, and Applications*, ed. TJ Cornwell, RA Perley, *ASP Conf. Ser.*, 19:281–88. San Francisco: Astron. Soc. Pac.
Roberts DH, Wardle JFC, Brown LF, Gabuzda DC, Cawthorne TV. 1990. See Zensus &

Pearson 1990, pp. 110–16
Roland J, Frossati G, Teyssier R. 1994. *Astron. Astrophys.* 290:364–70
Roland J, Teyssier R, Roos N. 1994. *Astron. Astrophys.* 290:357–63
Romney JD, Benson JM, Dhawan V, Kellermann KI, Vermeulen RC, Walker RC. 1995. *Proc. Natl. Acad. Sci. USA* 92:11360–63
Roos N. 1988. *Ap. J.* 334:95–103
Roos N, Kaastra JS, Hummel CA. 1993. *Ap. J.* 409:130–33
Rose WK, Beall JH, Guillory J, Kainer S. 1987. *Ap. J.* 314:95–102
Schalinski CJ, Witzel A, Hummel CA, Krichbaum TP, Quirrenbach A, Johnston KJ. 1992. In *Physics of Active Galactic Nuclei*, ed. WJ Duschl, SJ Wagner, pp. 589–91. Heidelberg: Springer-Verlag
Schalinski CJ, Witzel A, Krichbaum TP, Graham DA, Standke KJ, et al. 1994. See Zensus & Kellermann 1994, pp. 45–48
Scheuer PAG. 1974. *MNRAS* 166:513–28
Scheuer PAG, Readhead ACS. 1979. *Nature* 277:182–85
Schilizzi RT. 1995. See Zensus et al 1995b, pp. 397–408
Shaffer DB, Marscher AP. 1987. See Zensus & Pearson 1987, pp. 67–75
Shklovskii IS. 1963. *Sov. Astron.* 6:465–76
Simon RS, Hall J, Johnston KJ, Spencer JH, Waak JA, Mutel RL. 1988. *Ap. J.* 326:L5–L8
Sol H, Pelletier G, Asséo E. 1989. *MNRAS* 237:411–29
Spencer RE. 1994. See Zensus & Kellermann 1994, pp. 35–38
Steffen W, Zensus JA, Krichbaum TP, Witzel A, Qian SJ. 1995. *Astron. Astrophys.* 302:335–42
Taylor D, Dyson JE, Axon DJ, Pedlar A. 1989. *MNRAS* 240:487–99
Taylor GB, Readhead ACS, Pearson TJ. 1996. *Ap. J.* 463:95–104
Taylor GB, Vermeulen RC. 1996. *Ap. J. Lett.* 457:L69–L71
Taylor GB, Vermeulen RC, Pearson TJ, Readhead ACS, Henstock DR, et al. 1994. *Ap. J. Suppl.* 95:345–69
Thakkar DD, Xu W, Readhead ACS, Pearson TJ, Taylor GB, et al. 1995. *Ap. J. Suppl.* 98:33–40
Tingay SJ, Jauncey DL, Preston RA, Reynolds JE, Meier DL, et al. 1994. *Aust. J. Phys.* 47:619–24
Unwin SC, Davis RJ, Muxlow TWB. 1994a. See Zensus & Kellermann 1994, pp. 81–86
Unwin SC, Wehrle AE. 1992. *Ap. J.* 398:74–86
Unwin SC, Wehrle AE, Lobanov AP, Zensus JA, Madejski GM, et al. 1997. *Ap. J.* 480:596–606
Unwin SC, Wehrle AE, Urry CM, Gilmore DM, Barton EJ, et al. 1994b. *Ap. J.* 432:103–13
Urry CM, Padovani P. 1995. *PASP* 107:803–45
Valtaoja E, Valtonen M, eds. 1992. *Variability of Blazars*. Cambridge: Cambridge Univ. Press
Venturi T, Castaldini C, Cotton WD, Feretti L, Giovannini G, et al. 1995. *Ap. J.* 454:735–44
Venturi T, Readhead ACS, Marr JM, Backer DC. 1993. *Ap. J.* 411:552–64
Vermeulen RC. 1995. *Proc. Natl. Acad. Sci. USA* 92:11385–89
Vermeulen RC, Bernstein RA, Hough DH, Readhead ACS. 1993. *Ap. J.* 417:541–46
Vermeulen RC, Cohen MH. 1994. *Ap. J.* 430:467–94
Vermeulen RC, Readhead ACS, Backer DC. 1994. *Ap. J.* 430:L41–L44
Von Montigny C, Bertsch DL, Chiang J, Dingus BL, Esposito JA, et al. 1995. *Astron. Astrophys.* 299:680–88
Wagner SJ, Camenzind M, Dreissigacker O, Borgeest U, Britzen S, et al. 1995. *Astron. Astrophys.* 298:688–98
Wagner SJ, Witzel A. 1995. *Annu. Rev. Astron. Astrophys.* 33:163–97
Wagner SJ, Witzel A, Heidt J, Krichbaum TP, Quirrenbach A, et al. 1996. *Astron. J.* 111:2187–211
Walker RC, Benson JM, Unwin SC. 1987. *Ap. J.* 316:546–72
Walker RC, Romney JD, Benson JM. 1994. *Ap. J. Lett.* 430:L45–L48
Walker RC, Romney JD, Vermeulen RC, Dhawan V, Kellermann KI. 1996. See Ekers et al 1996, pp. 30–32
Wardle JFC, Cawthorne TV, Roberts DH, Brown LF. 1994. *Ap. J.* 437:122–35
Weatherall JC, Benford G. 1991. *Ap. J.* 378: 543–49
Wehrle AE, Cohen MH, Unwin SC, Aller HD, Aller MF, Nicolson G. 1992. *Ap. J.* 391:589–607
Wehrle AE, Unwin SC, Zook AC. 1994. See Zensus & Kellermann 1994, pp. 197–200
Wehrle AE, Unwin SC, Zook AC, Urry CM, Marscher AP, Teräsranta H. 1996. In *Blazar Continuum Variability*, ASP Conf. Ser. 110:430–35. San Francisco: Astron. Soc. Pac.
Wiita PJ. 1996. See Hardee et al 1996, pp. 395–404
Wilkinson PN. 1995. *Proc. Natl. Acad. Sci. USA* 92:11342–47
Witzel A, Schalinski CJ, Biermann PL, Krichbaum TP, Johnston KJ. 1988. *Astron. Astrophys.* 206:245–52
Xu W, Readhead ACS, Pearson TJ, Polatidis AG, Wilkinson PN. 1995. *Ap. J. Suppl.* 99:297–348
Xu W, Readhead ACS, Pearson TJ, Wilkinson PN, Polatidis AG. 1994. See Zensus & Kellermann 1994, pp. 7–10
Zensus JA, Biretta JA, Unwin SC, Cohen MH.

1990. *Astron. J.* 100:1777–84
Zensus JA, Cohen MH, Unwin SC. 1995a. *Ap. J.* 443:35–53
Zensus JA, Diamond PJ, Napier PJ, eds. 1995b. *Very Long Baseline Interferometry and the Very Long Baseline Array,* ASP Conf. Ser. 82. San Francisco: Astron. Soc. Pac.
Zensus JA, Kellermann KI, eds. 1994. *Compact Extragalactic Radio Sources.* Green Bank, WVa: Natl. Radio Astron. Obs.
Zensus JA, Krichbaum TP, Lobanov AP. 1995c. *Proc. Natl. Acad. Sci. USA* 92:11348–55
Zensus JA, Pearson TJ, eds. 1987. *Superluminal Radio Sources.* Cambridge: Cambridge Univ. Press
Zensus JA, Pearson TJ, eds. 1990. *Parsec-Scale Radio Jets.* Cambridge: Cambridge Univ. Press
Zensus JA, Porcas RW. 1987. See Zensus & Pearson 1987, pp. 126–28